IEEE Access
Multidisciplinary | Rapid Review | Open Access Journal

Received January 9, 2019, accepted January 23, 2019, date of publication January 31, 2019, date of current version February 14, 2019.

Digital Object Identifier 10.1109/ACCESS.2019.2895895

Detection of Sound Field Aberrations Caused by Forward Scattering From Underwater Intruders Using Unsupervised Machine Learning

BO LEI[1,2], (Member, IEEE), YAO ZHANG[1,2], AND YIXIN YANG[1,2], (Member, IEEE)
[1]School of Marine Science and Technology, Northwestern Polytechnical University, Xi'an 710072, China
[2]Key Laboratory of Ocean Acoustics and Sensing, Northwestern Polytechnical University, Ministry of Industry and Information Technology, Xi'an 710072, China

Corresponding author: Yixin Yang (yxyang@nwpu.edu.cn)

This work was supported in part by the National Natural Science Foundation of China under Grant 61571366, in part by the Fundamental Research Funds for the Central Universities under Grant 3102018AX003, and in part by the 111 Project under Grant B18041.

ABSTRACT Forward scattered waves are produced by underwater intruders that cross a source–receiver line. Strong direct blasts lead to a difficult detection of sound field aberrations caused by forward scattered waves. An unsupervised detection scheme that processes repeatedly transmitted pulses on a receiver array is proposed. For detection under strong blasts, the scheme performs unsupervised learning on spectra of normalized envelopes on an array output, which has the advantage of robustness for weak field aberrations and real-time detection after effective training. An experiment was carried out on the lake; the results show that the method has yielded reliable results in comparison with approximately 1-dB aberrations on the received pulse strengths caused by forward scattering from an intruder. Furthermore, the relationship between strength aberrations caused by forward scattering and the location of the intruder through the baseline is discussed further, and the capabilities of the scheme are further discussed with noise-added experimental data.

INDEX TERMS Forward scattering, littoral water, sound field aberration, unsupervised machine learning.

I. INTRODUCTION

Forward scattered waves are produced when an underwater intruder crosses the baseline between a source and a receiver. Sound field aberration occurs when a forward scattered wave arrives on the receiver and interferes with direct blasts. This aberration is intensely weak and difficult to detect because the strength of the direct blasts is several decibels over the forward scattered waves when the receiver is far from the target. Moreover, the dynamics of the environment can cause fluctuation on the received signal. The detection of the aberration produced by the forward scattered signal from the fluctuation caused by undulating environment directly without a priori knowledge is difficult.

Researchers have proposed several processing methods and techniques for detecting acoustic field aberrations. Gillespie *et al.* [1], Matveev and Mityugov [2], and Matveev *et al.* [3] proposed similar methods that adopted matched filtering techniques to detect perturbed fields; the effectiveness of the method was evaluated using models and data obtained from experiments in a lake. This processing technique was intuitive and preliminary. Folegot *et al.* [4] developed a localization algorithm based on forward scattering by using the result of an experiment set in a harbor. Song *et al.* [5] implemented an active time-reversal experiment and observed that field aberrations were initially observed with the increase in the intensity of side lobes near the focal zone. Sabra *et al.* [6] analyzed the stable portions of received pulses and extracted the aberrations of recorded signals on hydrophones using principal component analysis (PCA). At the laboratory scale, Marandet *et al.* [7] experimentally demonstrated the detection and localization of a wavelength-sized target in a shallow ultrasonic waveguide between two source–receiver arrays at 3 MHz. Lei *et al.* [8], [9] further combined PCA with array processing to enhance the aberrations of the recorded direct arrival data on a short vertical receiver array (VRA), validated the performance of the proposed method on the basis of a lake experiment, and identified the relationship between sound field aberration and crossing distance in theory

The associate editor coordinating the review of this manuscript and approving it for publication was Stavros Ntalampiras.

and experiment. The adaptive processing scheme and PCA-based concept are executed after acquiring several pulses. He *et al.* [10] proposed a processing scheme based on adaptive filtering to decrease the degree of received data association; Lei *et al.* [11] developed this technology to a dynamic environment and enhanced the forward scattered signal by 10 dB higher than the direct blasts.

Machine learning refers to programming computers to optimize a performance criterion using sample data or past experience [12]. In recent years, applying machine learning has achieved considerable results in many fields, such as speech recognition [13] and image processing [14]. In ocean acoustics, machine learning is preliminarily introduced in source localization [15], [16] and sediment density estimation [17]. Recently, Liu *et al.* [18], [19] proposed an unsupervised machine learning method called isolation forest (*i*Forest) for anomaly detection. *i*Forest builds an ensemble of isolation trees (*i*Trees) for a given data set, and anomalies are instances with short average path lengths on *i*Trees. This method detects anomalies purely on the basis of the concept of isolation without using any distance or density measurement. Furthermore, this method has been verified to work effectively in high-dimensional problems that contain several irrelevant attributes. Under the forward scattering detection configuration, a pulse signal is transmitted repeatedly and successively. The field aberration caused by forward scattering from intruders can be considered the anomalies of strength and arrival structure on the receivers. Thus, the received signal that contains forward scattered waves can be considered an abnormality with respect to direct blasts.

Therefore, a scheme based on this unsupervised machine learning concept for forward scattering detection is proposed. The received waveforms were subjected to a feature extraction process to suppress the variation in the received signal caused by environment undulations. A lake experiment, in which a sinusoidal signal with 10 cycles was transmitted repeatedly and received by a VRA placed in the water column, was conducted. The scheme performed effectively on the experimental data. The well-trained intruder might be detected nearly in real time.

The remainder of this paper is organized as follows. Section II provides the principle of the scheme based on unsupervised machine learning. Section III describes the experimental configuration and illustrates the processed results. Section IV discusses the performance with different signal-to-noise ratios (SNRs). Section V presents the conclusions of this study.

II. DETECTION BASED ON UNSUPERVISED MACHINE LEARNING

Forward scattering detection is a specified configuration in a bistatic sonar system, which constantly broadcasts signals successively and pulses repeatedly. When a submerged object invades an area between the sound source and the receiver because of forward scattering, an extremely weak sound field aberration occurs on the receiver at an extended distance. Therefore, intruders can be alerted by detecting this sound field aberration.

The problem of detecting the field aberration can be transformed into a problem of detecting anomalies. For a data set, ungrouped data points are anomalies. In detecting sound field aberration caused by forward scattering, a direct blast pulse is dominant, and the similarity can be considered normal. The field aberrations caused by the forward scattering are minor and isolated. These results can be regarded as abnormalities. In *i*Forests, the attribute space spanned by the attributes of data set is continuously segmented with hyperplanes until each subspace contains only one data point. The direct blast pulses are concentrated in the attribute space and must be split multiple times to be isolated. The pulses affected by the forward scattering are scattered, drawn out of the group in the data space, and can be isolated only with a small number of divisions. Therefore, anomaly detection can be achieved by analyzing the difficulty of isolated data points.

Under the forward scattering configuration, the amplitude of the received signal disturbed by the forward scattering from intruders may be slight when the receiver is far from the intruder. In practice, the anomaly may also be caused by interference and environmental disturbances in addition to the forward scattered signal, thereby causing a serious problem when anomaly detection is utilized to detect the intruder with forward scattering. Many literature [8], [10] reviews have shown that beamforming on a vertical hydrophone array can suppress a multipath direct blast and enhance the forward scattered signal–direct blast ratio. The present study further compares the detection performance of a beam output that steered to horizontal direction and a single hydrophone and draws a consistent conclusion.

A feature extraction process is required to ensure that the detection method is stable and has favorable generalization capabilities. The Hilbert transform on the received signals was initially executed to obtain the pressure strength and then normalized by a signal power to eliminate the influence of attenuation in a time-varying channel. Discrete Fourier transform (DFT) was then executed on the normalized envelope waveforms because using the spectrum as the feature vector of the algorithm avoids the instability of the time domain waveform. The spectrum of the normalized envelope is expressed as follows:

$$\mathbf{X}(f) = [x_1(f), x_2(f), \ldots, x_N(f)], \tag{1}$$

where f is the frequency, and $x_n(f)$ is the envelope spectrum of the nth received pulse signal (referred to as pulse envelope spectrum thereafter). $\mathrm{X}(f)$ with a dimension of $L \times N$ is used as input data for processing, where L is the length of a single pulse envelope spectrum, and N is the number of pulse envelope spectra. The two processing steps, namely, training and evaluation processes are executed within the *i*Forest algorithm to detect the field aberration caused by forward scattering from intruders. The training process uses training data to build *i*Trees, whereas the evaluation process obtains an anomaly score for each pulse envelope spectrum.

Data set $\mathbf{X}$ includes the training data in the training process. A sub-sample of dimension $L \times \tilde{N}(\tilde{N} \leq N)$ selected randomly from $\mathbf{X}$ is used to build one an *i*Tree, which is denoted as $\tilde{\mathbf{X}}$. Frequency bin qth is selected randomly from $\boldsymbol{L}$ frequency bins for one *i*Tree. T denotes a node of an *i*Tree. Split value p between the max and min amplitudes of frequency bin q is randomly selected for node T. At node T, a test $\tilde{\mathbf{X}}(q) > p$ or $\tilde{\mathbf{X}}(q) < p$ determines the traversal of pulse envelope spectra $x_i \in \tilde{\mathbf{X}}$ to either T_l or T_r, the two daughter nodes of T. These steps are repeated until $\tilde{N}$ pulse envelope spectra are isolated (the last node has only one pulse envelope spectrum, or all pulse envelope spectra at the node have the same amplitudes) or have reached the height limit of the *i*Trees to complete one *i*Tree. The height limit defaults to $hlim = \log_2(\tilde{N})$ to ensure algorithm efficiency. Multiple *i*Trees are created by repeating these steps. At the end of the training process, a collection of *i*Trees is returned for evaluation.

In the evaluation procedure, the test spectra are processed through *i*Trees to obtain an anomaly score for each pulse. The test spectra travel along the corresponding branch in the *i*Tree until the external node is reached. The path length $h(x)$ that was passed during this process is recorded. The path length $h(x)$ indicates the number of edges that passed when a pulse envelope spectrum x traverses from the root node through an intermediate node and finally reaches an external node in an *i*Tree, and its value indicates the anomaly level of pulse envelope spectra. A short path length indicates a high susceptibility to isolation, and its counterpart indicates a low susceptibility. Therefore, the spectra disturbed by forward scattering must have short path lengths because they are highly decentralized, i.e., more isolated than other spectra in the data space. Isolated data are separated from other data early on *i*Trees.

An anomaly score for pulse envelope spectrum x is defined as follows:

$$\mathrm{s}(x, \tilde{N}) = 2^{-E(h(x))/a(\tilde{N})}, \tag{2}$$

where $E(h(x))$ is the average of $h(x)$ from a collection of *i*Trees. $a(\tilde{N})$ is the average of $h(x)$ with a given $\tilde{N}$ expressed as follows:

$$a\left(\tilde{N}\right) = \begin{cases} 2H\left(\tilde{N}-1\right) - 2\left(\tilde{N}-1\right)/\tilde{N} & \text{for } \tilde{N} > 2 \\ 1 & \text{for } \tilde{N} = 2 \\ 0 & \text{for } \tilde{N} = 1, \end{cases} \tag{3}$$

where $H(i)$ is the harmonic number and can be estimated by $H(i) = \ln(i) + \xi$ (where $\xi \approx 0.5772156649$ is Euler's constant). In the application of anomaly detection, the data set with only one sample ($\tilde{N} = 1$) has no anomaly concept. Therefore, in this paper, $\tilde{N} \geq 2$ is required and thus $a\left(\tilde{N}\right) = 0$ does not actually occur.

Two limit values of the anomaly score are observed. (1) If the intruder is absent, then all the direct blasts are basically the same. The received pulses are concentrated in the data space, thereby resulting in scores at approximately 0.5. (2) If the intruder is present and the pulses disturbed by forward scattering are sufficiently isolated from other pulses in the data space, then the scores of these pulses will be approximately 1 and that of the other pulses will be nearly 0. Provided that the direct blast is much stronger than the forward scattered waves in detecting sound field aberrations, the scores for the received signals that contain a forward scattered signal and that of received signals that only contain direct blasts may not have an apparent difference. The following experimental results corroborate that the scores for a received signal that contains a forward scattered wave reach 0.6 and that the scores for only the direct blast are approximately 0.4.

Since the normalization in the feature extraction process results in the loss of the amplitude information, the anomaly score s needs to be compensated as follows:

$$\Delta M = \frac{M}{E(M)}, \tag{4}$$

$$s' = (1 + |\Delta M - 1|) \times s, \tag{5}$$

where M is the maximum amplitude of the received pulse signal, and $E(M)$ is the average maximum amplitude calculated by the maximum amplitude of the received pulses in the previous 100 s.

The processing procedures for the proposed scheme are illustrated in Figure 1 and described as follows:

Step 1. Feature extraction processing. The received signals undergo Hilbert transform to obtain the envelopes and are then normalized by power. DFT is then applied to obtain the spectra. Finally, the processing frequency band is intercepted on the basis of the frequency band of transmitted signal envelopes.

Step 2. The input data are divided into training and testing data, or all the data are used as training and testing data because *i*Forest is an unsupervised machine learning algorithm. The training data do not require being labeled. Thus, *a priori* knowledge of data anomaly is superfluous.

Step 3. Training data are used to build *i*Trees.

Step 4. The anomaly scores for each pulse are obtained using (5). Thereafter, sound field aberrations may be detected in accordance with anomaly scores.

A receiver operating characteristic (ROC) [20] curve is a graphical plot that illustrates the diagnostic ability of a binary classifier system because its discrimination threshold varies. A pulse that is accurately predicted to be affected by a forward scattered signal is called true positive (TP); otherwise, it is called false positive (FP). Similarly, a pulse that is accurately predicted to be a regular pulse is called true negative (TN); otherwise, it is called false negative (FN). The TP rate (*TPR*) and FP rate (*FPR*) are defined as follows:

$$TPR = \frac{TP}{TP + FN}, \tag{6}$$

$$FPR = \frac{FP}{TN + FP}, \tag{7}$$

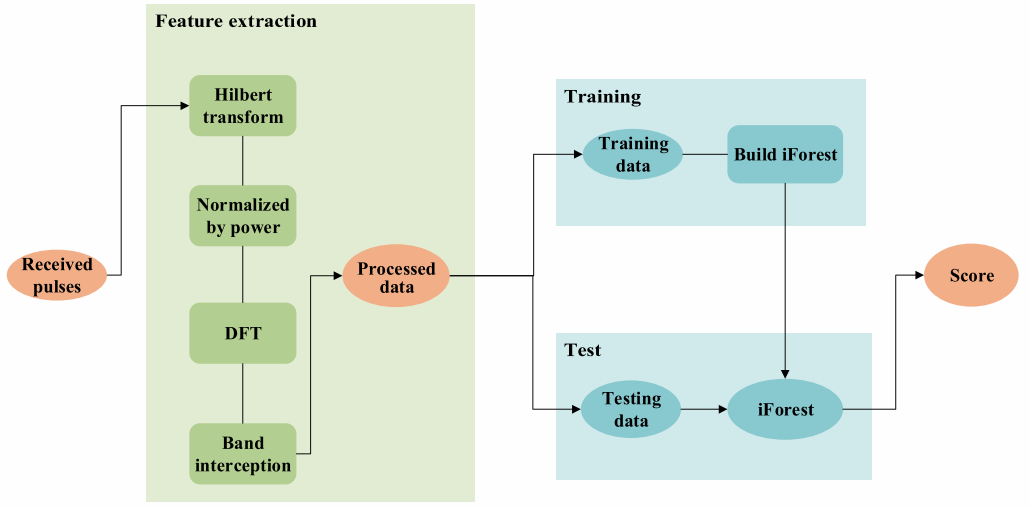

FIGURE 1. Detection scheme within four steps. Step 1. The received signals undergo Hilbert transform to obtain the envelope and are then normalized by power. DFT is then applied to obtain the spectra. Step 2. The input data are divided into training and testing data. Step 3. The training data are used to build *i* Trees. Step 4. The anomaly scores for each pulse envelope spectrum are obtained.

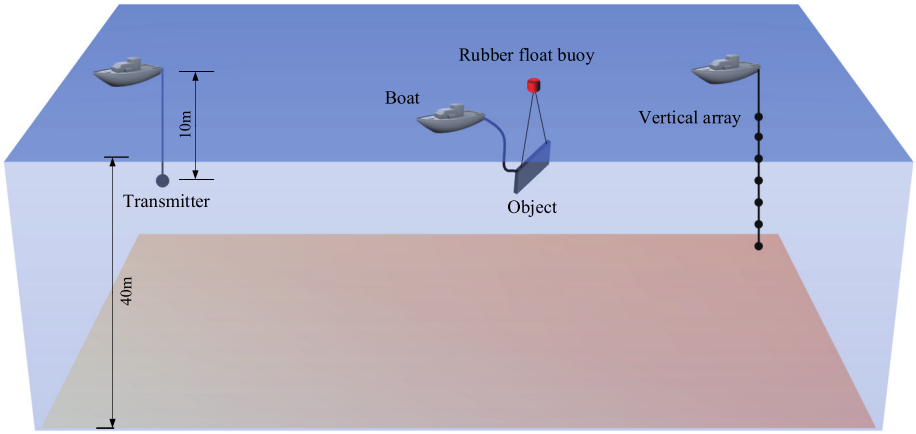

FIGURE 2. Experimental setup in the lake. The depth was 40 m, and the source–receiver range was 1100 m. The source, object and receiver were placed at a depth of 10m and the intruder was towed 15 m behind a boat that travelled approximately perpendicularly to the source–receiver line.

where *TP*,*FP*, *TN*, and *FN* are the positive or negative numbers of the four cases. The ROC curve is created by plotting the TPR against the FPR at various threshold settings. The area under the ROC curve (frequently referred to as simply the AUC) [21] is equal to the probability that a classifier will rank a randomly selected positive instance higher than a randomly selected negative one (assuming that ''positive'' ranks higher than ''negative''). An AUC value that is approximately 1 indicates an effective detection effect. Calculating the AUC is to calculate the area between the ROC and the abscissa axis. Assuming that the ROC is formed by a series of point connections with coordinates $\{(A_1, B_1), (A_2, B_2), \cdots, (A_m, B_m)\}$, the AUC can be estimated as:

$$AUC = \frac{1}{2}\sum_{i=1}^{m-1}(A_{i+1} - B_i)(A_i + B_{i+1}) \tag{8}$$

III. EXPERIMENT AND PROCESSING RESULTS

In Figure 2, an experiment was conducted in a lake with a depth of 40 m. An omnidirectional transmitter with a resonance frequency of 11 kHz was deployed at a depth of 10 m, and a VRA that included 13 omnidirectional hydrophones was positioned. The center of the array was at the same depth with the source, and the inter-sensor spacing was 25 cm. The distance between the source and the VRA was 1100 m, which is in accordance with the global positioning system measurement. A plastic foam plate (length = 6 m; width = 2 m; thickness = 5 cm), covered on both sides by aluminum plates, was submerged into the line between the source and the VRA. A load was attached beneath the object to provide negative buoyancy. The object was centered at an approximate depth of 10 m. The source intermittently transmits a pulse signal to reduce aliasing of the multipath propagation signal. A 0.5 ms sinusoidal pulse was transmitted repeatedly every 0.5 s at a

frequency of 10 kHz, and the sampling frequency was set to 223 kHz on the receivers.

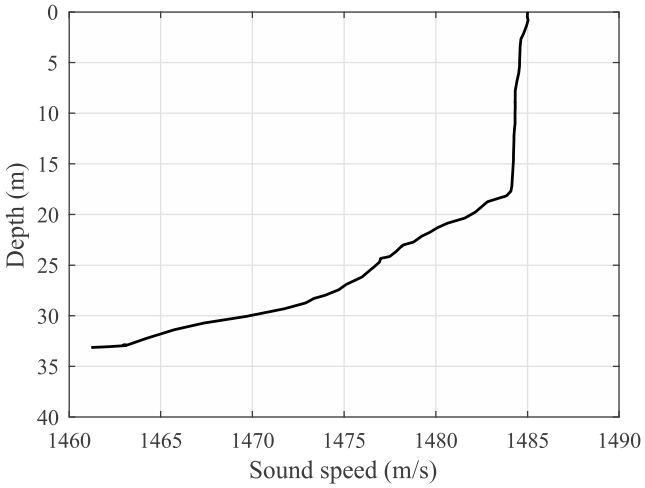

FIGURE 3. Sound speed profile. The upper volume was an isovelocity and the sound speed was approximately 1484 m/s. The sound speed profile has a negative gradient at the low volume.

The sound speed profile was measured with conductivity-temperature-depth instrument (CTD), as depicted in Figure 3. The upper volume was an isovelocity, and the sound speed was approximately 1484 m/s. The sound speed profile was a negative gradient at the low volume given the temperature decrease. The depth of the sound speed was 33 m because we did not have the exact information beyond the bottom. At the lowest volume, the sound speed, which was evaluated in accordance with the negative gradient, was approximately 1445 m/s at the depth of 40 m. The bottom was assumed to be a half-space with a density of 1.6 g/cm3 and sound speed of 1720 m/s.

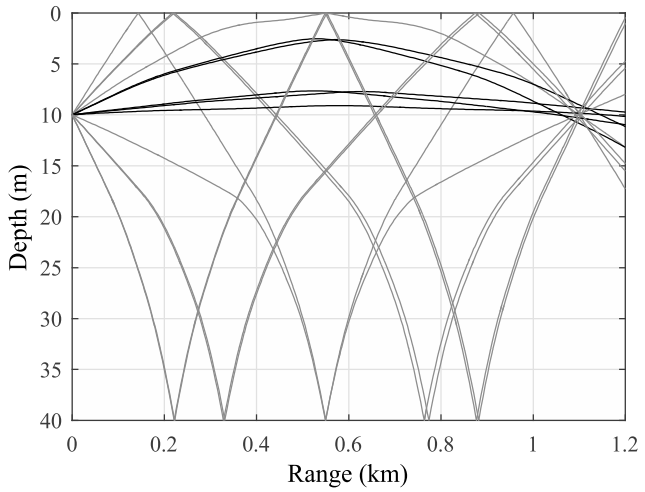

FIGURE 4. Eigenrays in the experimental environment simulated by the bellhop ray model. The Figure does not include ray that bounces more than twice between the surface and the floor. It shows that the main energy is horizontally oriented.

The sound propagation under the experimental environment is simulated using the bellhop ray model [22], [23], and the eigenrays are demonstrated in Figure 4 (excluding more than two bounces on the surface or seafloor). The propagation path results showed that the main energy is horizontally oriented. Thus, the VRA was subjected to Chebyshev time-delay beamforming with the beam steered to the hydrophone array broadside. The array horizontal beam output waveform is compared with the waveform of a single hydrophone, as exhibited in Figure 5. The horizontal direct blasts and the blasts from the bottom reflections are partially amplified. The left panel clearly shows that the direct blasts remain intact in the beam output, whereas the blasts from the bottom reflections in the right panel are effectively suppressed in the beam output. In the following context, the detection results obtained from the output of a single hydrophone and the horizontally steered beam output were further discussed.

The intruder was towed 15 m behind a boat that travels approximately perpendicularly to the source–receiver line at a distance of 186 m (hereinafter referred to as Case 1) and 324 m (hereinafter referred to as Case 2) from the VRA. The strength aberrations of the received pulses on the output of beam steered to horizontal for two cases are plotted in Figures 6(a) and 6(d), respectively. The sound field aberration caused by forward scattering could be weakly observed between 100 and 140 s. The strength aberrations of received signals were not more than 3 dB in Figure 6(a) and approximately 1 dB in Figure 6(d). The bandwidth of the envelope spectrum was 2 kHz because the length of one pulse was 0.5 ms. Therefore, the frequency band below 2 kHz was intercepted to reduce extraneous frequency response bins and suppress noise. After feature extraction processing, each pulse envelope spectrum contained 93 equally spaced frequency response bins, i.e., 93 features. Therefore, the input samples were 93-dimensional. A high dimension is an important factor for selecting the *i*Forest algorithm. The data above were used as the training data to build the *i*Forest.

The path lengths in the *i*Forest algorithm typically converge effectively before 100 *i*Trees according to Liu's research result. Therefore, the *i*Forest performed in this study included 100 *i*Trees. For each *i*Tree, subsampling size $\tilde{N}$ is set to 256 according to Liu's research. Thus, the height limit for the*i*Trees was set to 8.

Once *i*Forest is performed, the anomaly scores for each pulse can be obtained using (2). Figure 6(b) exhibits the anomaly scores for the data shown in Figure 6(a). At a running time of approximately 95–150 s, the object crossed through the source–receiver line. Thus, forward scattering occurred, and the scores were significant at higher than 0.6. For direct blasts, the scores were mostly close to 0.4. At a running time of approximately 75 and 165 s, the scores were higher than 0.5 for a few pulses. These high scores might be caused by an interference from the experimental environment or equipment. The results showed that the proposed scheme can effectively distinguish the sound field aberration caused by forward scattering even under strong direct blasts.

When underwater intruders cross the line at a far distance from the receiver, The strength aberrations of the received pulses on the output of beam steered to horizontal are plotted in Figure 6(d). The forward scattered waves are weaker than the short-range forward scattered waves because the

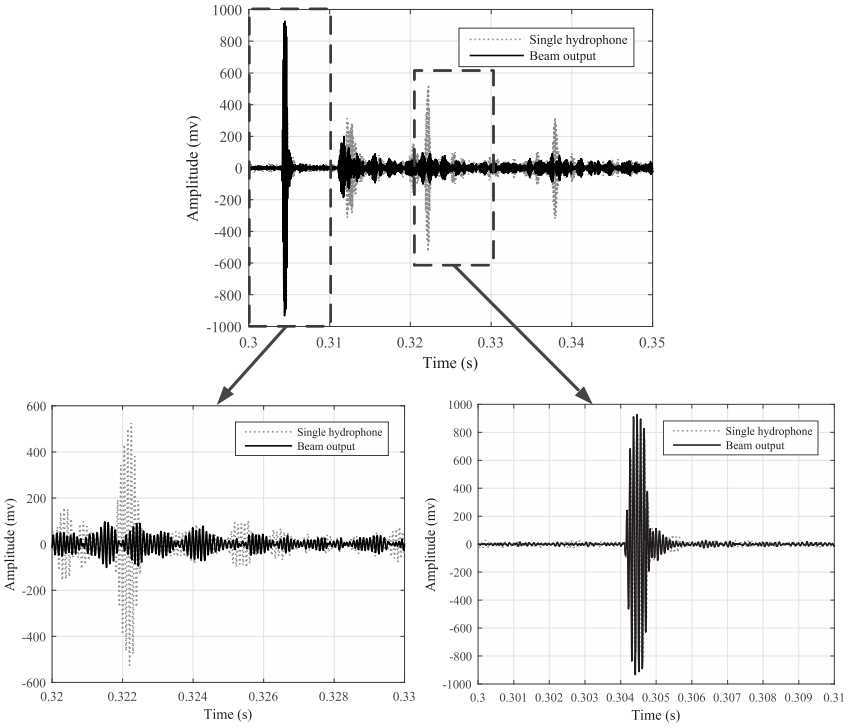

FIGURE 5. Waveforms of the array horizontal beam output and a single hydrophone. The horizontal direct blasts and the blasts from the bottom reflections are partially amplified. The left panel clearly shows that the direct blasts remain intact in the beam output, whereas the blasts from the bottom reflections observed in the right panel are effectively suppressed in the beam output.

underwater intruders cross the source–receiver line farther from the receiver. In this case, detecting the intruders was difficult. Nearly no sound field aberration can be directly found in Figure 6(d). The anomaly scores of data is displayed in Figure 6(e), in which the anomaly scores of the pulse envelope spectra affected by forward scattering generally reached 0.6, whereas the score of the direct blast was approximately 0.4. This result confirmed that the weak sound field aberration in this set of data remains successfully detected as an outlier. The ROC curve of the detection result presented in Figure 6(b) is illustrated in Figure 6(c). The AUC for the beam output and single hydrophone is 0.94 and 0.85, correspondingly. The ROC curve of the detection result demonstrated in Figure 6(e) is depicted in Figure 6(f). The AUC for the beam output is 0.81 and that for the single hydrophone signal is 0.74. Evidently, the detection performance declined when intruders pass through the source–receiver line at long ranges given the weak forward scattered waves, but it could still be maintained at a high level. The result from the array was remarkably better than that of the single hydrophone, thus indicating that the beamforming on the vertical array effectively suppresses the abnormalities caused by other interferences that lead to FPs. Therefore, horizontal beamforming output signals are used in the following demonstrations.

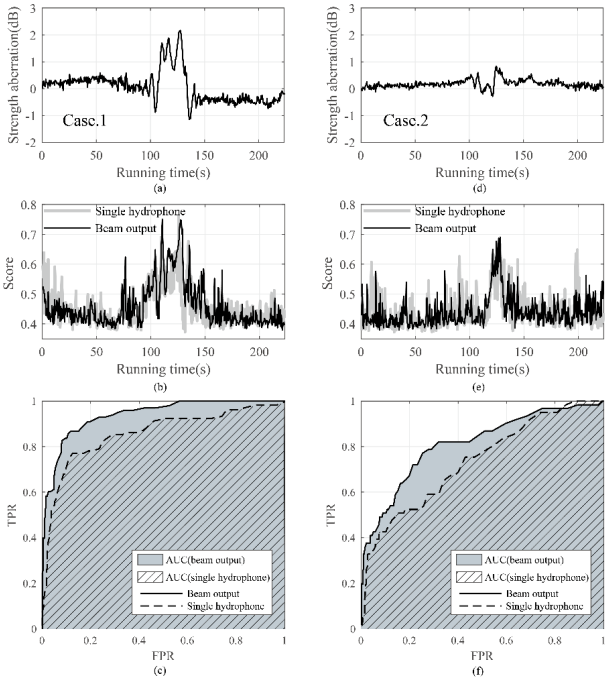

FIGURE 6. Processed results on the experimental data. Panels (a) and (d) show the strength aberrations of received pulse obtained from the output of beam steered to horizontal for Case 1 and Case 2, respectively. In Panels (b) and (e), the dark and light lines show the score of each pulse in Panels (a) and (d), correspondingly. Panels (c) and (f) show the ROC curves for the detection results of Case 1 and Case 2, respectively.

IV. DISCUSSIONS

For the forward scattering detection system, the sonar equation associated with the difference between forward scattered signal and direct blast strengths can be used for performance estimation and is derived using the following equation. In the littoral waveguide, the transmission loss (TL) can be

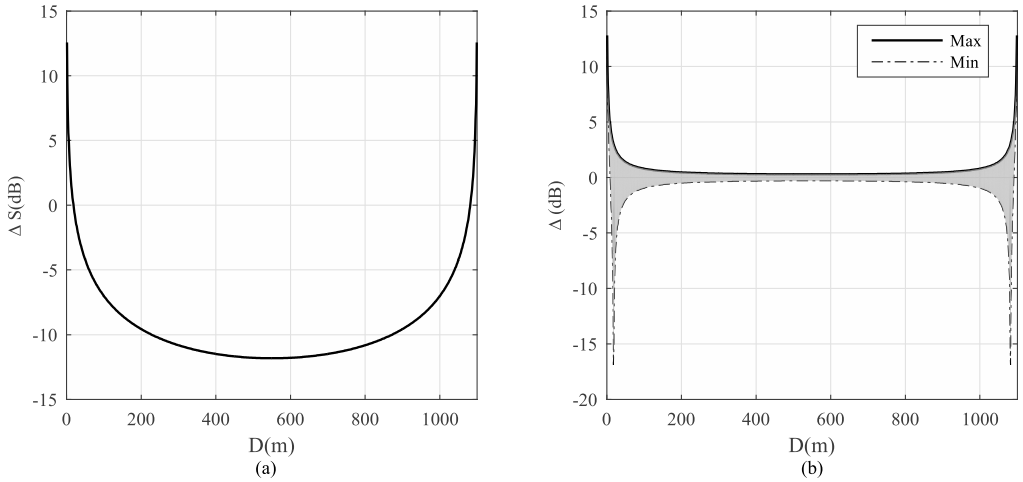

FIGURE 7. Panel (a) shows the relationship between distance and forward scattered signal–direct blast ratio. A crossing point that is close to the midpoint of the baseline implies that a weak forward scattered signal–direct blast ratio. Panel (b) shows the range of values for the strength aberrations at different distances.

evaluated using the following equation [24]:

$$\mathrm{TL}(R) = 20\log_{10} R_0 + 10\log_{10}(R/R_0) + \alpha R, \tag{9}$$

$$R_0 = \frac{H}{2\tan\beta_0}, \tag{10}$$

where H is the water depth for the waveguide, R is the source–receiver range, α is the waveguide absorption loss in decibels per kilometer, and β_0 is the critical angle on the fluid bottom. The SNR for the direct blast can be estimated as follows:

$$\mathrm{SNR}_0 = \mathrm{SL} - \mathrm{TL}(R) + \mathrm{DI} - \mathrm{NL}, \tag{11}$$

where SL is the source level, NL is the noise level, and DI is the directivity index. The SNR for an intruder with a target strength (TS) that crosses a distance D away from the receiver is expressed using the following equation:

$$\mathrm{SNR} = \mathrm{SL} - \mathrm{TL}(R-D) - \mathrm{TL}(D) + \mathrm{TS} + \mathrm{DI} - \mathrm{NL}. \tag{12}$$

The forward TS associated with the projected cross-section area A and wavelength λ can be approximated by the following formula [25]:

$$\mathrm{TS} = 20\log_{10}(A/\lambda), \tag{13}$$

The TS in an ocean waveguide might be smaller than its value in a free space given the presence of absorption in the medium [26]. If the NL is assumed to remain constant during the crossing of the target, the forward scattered signal–direct blast ratio ΔS can be approximated as follows:

$$\begin{aligned}\Delta S &= \mathrm{SNR} - \mathrm{SNR}_0 \\ &= \mathrm{TS} + 10\log_{10}\left(\frac{R}{D(R-D)}\right) - 10\log_{10} R_0.\end{aligned} \tag{14}$$

For the experimental environment and target used in the experiment ($A = 12$ m^2, $\lambda = 0.15$ m, and TS$\approx$38 dB), the relationship between D and ΔS is displayed in Figure 7(a). A crossing point that is close to the midpoint of the baseline indicates a weak received forward scattered waves. The strength aberrations Δ of received signals caused by forward scattering can be approximated as follows:

$$\begin{aligned}\Delta_{\max} &= 10\log_{10}\left(1 + 10^{\frac{\Delta S}{10}}\right) \\ \Delta_{\min} &= 10\log_{10}\left(\left|1 - 10^{\frac{\Delta S}{10}}\right|\right).\end{aligned} \tag{15}$$

The range of values for the strength aberrations Δ at different distances D is presented in Figure 7(b).

In this process, the same data set was performed for training and testing because the experimental data are limited. Therefore, this process is similar to the post-processing scheme. However, because the intruder is moving, the real-time detection is practical in applications. Gaussian white noise with a limited bandwidth of 4 kHz (transmitted signal frequency band) is added to the received signal of each hydrophone with an SNR of 10 dB (the SNR is based on the estimated energy of forward scattered waves in accordance with (14)) due to the limited amount of the experimental data to simulate the effect of the dynamic environment on the amplitude of the received signal. Thus, the testing data are different from the training data. The noise-added data are used as the new test data and subjected to feature extraction processing, and the strength aberrations for new test data illustrated in Figures 8(a) and 8(d). Monte Carlo simulations are run for 500 times. The proposed method can also detect the sound field aberration from this noise-added data, and the averaged anomaly scores are depicted in Figures 8(b) and 8(e). In comparison with the results demonstrated in Figures 6(b) and 6(e), the anomaly scores generally increased because the noise-added data are more isolated compared with the original data. Therefore, with the difference between the test data and the training data expanding, the detection threshold needs to be appropriately increased. The anomaly scores of the pulse envelope spectra affected

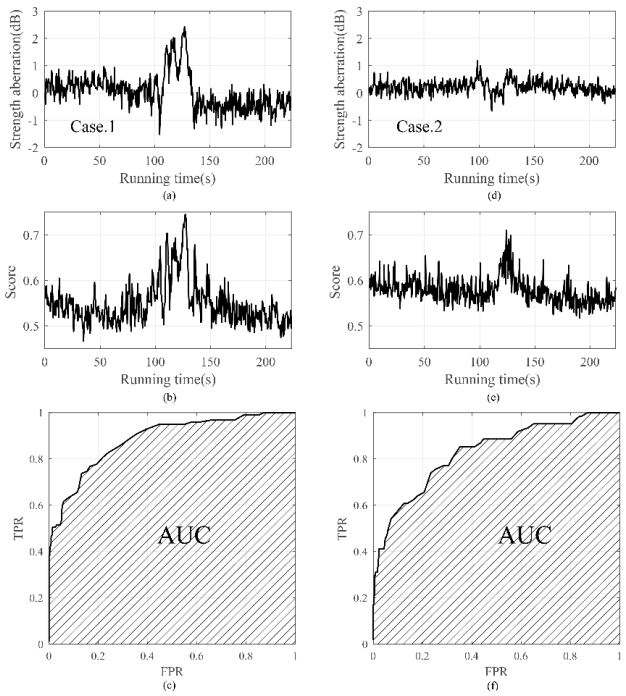

FIGURE 8. Processed results on the experimental data with added Gaussian noise. Panels (a) and (d) are strength aberrations of normalized noise-added signals that correspond to the signals displayed in Figures 6(a) and 6(d), respectively. Panels (b) and (e) show the average score of each pulse in Panels (a) and (d) after 500 Monte Carlo runs, correspondingly. Panel (c) shows the ROC curve for the detection results of Case 1, and Panel (f) shows the ROC curve for the detection results of Case 2. Panels (c) and (f) show the ROC curves for the detection results of Case 1 and Case 2 for 500 Monte Carlo runs.

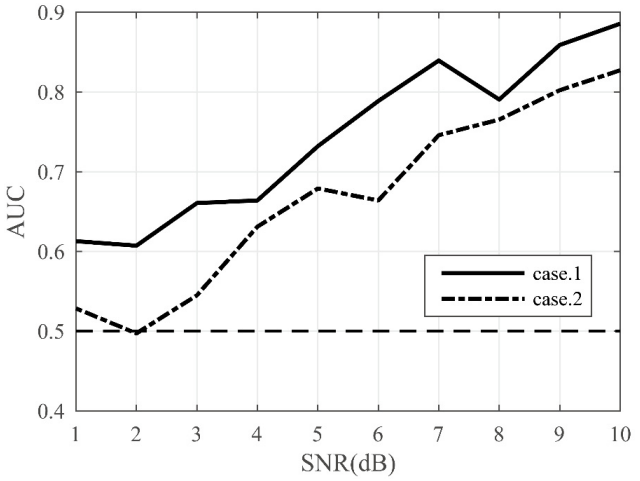

FIGURE 9. AUC for different SNRs. Inconsistent signal-to-noise ratios between training data and test data can cause performance degradation, and detector performances approach the performance of random detectors at low signal-to-noise ratios.

by forward scattering were generally higher than direct pulse by 0.1 $\sim$ 0.2, which is lower than the difference of 0.3 in Figures 6(b) and 6(e). This indicates a decrease in detection performance. The ROC curves are illustrated in Figures 8(c) and 8(f). The AUCs of the received data are 0.89 and 0.83 in the two cases when the intruder is close to the source–receiver line.

The AUCs under different SNRs are depicted in Figure 9. The detection performance gradually decreases, and the AUC gradually approaches 0.5 with the decrease in SNR. The random detector has an AUC of 0.5; thus, a detector with an AUC higher than 0.5 is valuable. The results show that the inconsistency of the signal-to-noise ratio of the training data and the test data leads to a decline in detection performance.

V. CONCLUSIONS

The problem of underwater detection using sound field aberrations is interesting. However, this detection is a challenge due to weak aberrations caused by a strong direct blast interference. This study presents a simple, robust, and data-based method that addresses the problem.

This method is not dedicated to extracting or amplifying the characteristics of the forward scattered signal but to providing a real-time detection that relies only on the weak effects generated by the forward scattered signals. The method uses small-scale, unlabeled data for training to divide a data space into normal and anomalous data spaces. The normalized envelope spectrum is designed to achieve a robust method in a fluctuating environment. Notably, this method enables real-time detection after training. The application of measured data shows that the detection is successful when the sound field aberration is approximately 1 dB under the interference of a strong direct blast. Moreover, when the crossing point between an intruder and a source–receiver line is close to the receivers, the possibilities of detection are high because the strength of field aberration is evident in accordance with the proposed sonar equation.

The size of the data used in this study is on the order of hundreds. When additional experimental data are provided, the proposed method may achieve remarkable results. In addition, the data, which only include the undulating direct blasts, may be utilized for training.

REFERENCES

[1] B. Gillespie, K. Rolt, G. Edelson, R. Shaffer, and P. Hursky, "Littoral target forward scattering," in *Acoustical Imaging*, vol. 23, S. Lees and L. A. Ferrari, Eds. Boston, MA, USA: Springer, 1997, pp. 501–506.

[2] A. L. Matveev and V. V. Mityugov, "Complex matched filtering of diffraction sound signals received by a vertical array," *Acoust. Phys.*, vol. 46, no. 1, pp. 80–86, 2000.

[3] A. L. Matveev, R. C. Spindel, and D. Rouseff, "Forward scattering observation with partially coherent spatial processing of vertical array signals in shallow water," *IEEE J. Ocean. Eng.*, vol. 32, no. 3, pp. 626–639, Jul. 2007.

[4] T. Folegot, G. Martinelli, P. Guerrini, and J. M. Stevenson, "An active acoustic tripwire for simultaneous detection and localization of multiple underwater intruders," *J. Acoust. Soc. Amer.*, vol. 124, no. 5, pp. 2852–2860, 2008.

[5] H. Song, W. A. Kuperman, W. S. Hodgkiss, T. Akal, and P. Guerrini, "Demonstration of a high-frequency acoustic barrier with a time-reversal mirror," *IEEE J. Ocean. Eng.*, vol. 28, no. 2, pp. 246–249, Apr. 2003.

[6] K. G. Sabra *et al.*, "Experimental demonstration of a high-frequency forward scattering acoustic barrier in a dynamic coastal environment," *J. Acoust. Soc. Amer.*, vol. 127, no. 6, pp. 3430–3439, 2010.

[7] C. Marandet, P. Roux, B. Nicolas, and J. Mars, "Target detection and localization in shallow water: An experimental demonstration of the acoustic barrier problem at the laboratory scale," *J. Acoust. Soc. Amer.*, vol. 129, no. 1, p. 85, 2011.
[8] B. Lei, K. Yang, and Y. Ma, "Forward scattering detection of a submerged object by a vertical hydrophone array," *J. Acoust. Soc. Amer.*, vol. 136, no. 6, p. 2998, 2014.
[9] B. Lei, K. Yang, Y. Ma, and L. Wang, "Forward acoustic scattering by moving objects: Theory and experiment," *Chin. Sci. Bull.*, vol. 57, no. 4, pp. 313–319, 2012.
[10] C. He, K. Yang, B. Lei, and Y. Ma, "Forward scattering detection of a submerged moving target based on adaptive filtering technique," *J. Acoust. Soc. Amer.*, vol. 138, no. 3, pp. EL293–EL298, 2015.
[11] B. Lei, Y. Yang, K. Yang, and Y. Ma, "Detection of forward scattering from an intruder in a dynamic littoral environment," *J. Acoust. Soc. Amer.*, vol. 141, no. 3, p. 1704, 2017.
[12] T. Mitchell, B. Buchanan, G. DeJong, T. Dietterich, P. Rosenbloom, and A. Waibel, "Machine Learning," *Annu. Rev. Comput. Sci.*, vol. 4, no. 1, pp. 417–433, 1990.
[13] L. Deng and X. Li, "Machine learning paradigms for speech recognition: An overview," *IEEE Trans. Audio, Speech, Language Process.*, vol. 21, no. 5, pp. 1060–1089, May 2013.
[14] A. Krizhevsky, I. Sutskever, and G. E. Hinton, "ImageNet classification with deep convolutional neural networks," in *Proc. Int. Conf. Neural Inf. Process. Syst.*, 2012, pp. 1097–1105.
[15] H. Niu, E. Reeves, and P. Gerstoft, "Source localization in an ocean waveguide using supervised machine learning," *J. Acoust. Soc. Amer.*, vol. 142, no. 3, p. 1176, 2017.
[16] B. Z. Steinberg, M. J. Beran, S. H. Chin, and J. H. Howard, Jr., "A neural network approach to source localization," *J. Acoust. Soc. Amer.*, vol. 90, no. 4, pp. 2081–2090, 1991.
[17] A. Caiti and T. Parisini, "Mapping ocean sediments by RBF networks," *IEEE J. Ocean. Eng.*, vol. 19, no. 4, pp. 577–582, Oct. 1994.
[18] F. T. Liu, k. M. Ting, and Z.-H. Zhou, "Isolation Forest," in *Proc. 8th IEEE Int. Conf. Data Mining*, Dec. 2009, pp. 413–422.
[19] F. T. Liu, K. M. Ting, and Z. Zhou, "Isolation-based anomaly detection," *ACM Trans. Knowl. Discovery from Data*, vol. 6, no. 1, pp. 1–39, Mar. 2012.
[20] K. A. Spackman, "Signal detection theory: Valuable tools for evaluating inductive learning," in *Proc. 6th Int. Workshop Mach. Learn.*, A. M. Segre, Ed. San Francisco, CA, USA: Morgan Kaufmann, 1989, pp. 160–163.
[21] A. P. Bradley, "The use of the area under the ROC curve in the evaluation of machine learning algorithms," *Pattern Recognit.*, vol. 30, no. 7, pp. 1145–1159, 1997.
[22] F. B. Jensen, W. A. Kuperman, M. B. Porter, and H. Schmidt, *Computational Ocean Acoustics*. New York, NY, USA: Springer-Verlag, 2000, pp. 141–190.
[23] M. B. Porter and H. P. Bucker, " Gaussian beam tracing for computing ocean acoustic fields," *J. Acoust. Soc. Amer.*, vol. 82, no. 4, pp. 1349–1359, 1987.
[24] R. I. Odom, "An introduction to underwater acoustics: Principles and applications," *EOS Trans. Amer. Geophys. Union*, vol. 84, no. 28, p. 265, 2013.
[25] J. J. Bowman, T. B. A. Senior, and P. L. E. Uslenghi, *Electromagnetic Scattering by Simple Shapes*. New York, NY, USA: Hemisphere Publishing Corporation, 1969, pp. 349–588.
[26] P. Ratilal and N. C. Makris, "Extinction theorem for object scattering in a stratified medium," *J. Acoust. Soc. Amer.*, vol. 110, no. 6, pp. 2924–2945, 2001.

BO LEI (M'07) received the B.S. degree in electronic and information engineering and the M.S. and Ph.D. degrees in underwater acoustic engineering from Northwestern Polytechnical University (NPU), Xi'an, China, in 2004, 2007, and 2010, respectively.

From 2010 to 2012, he was a Postdoctoral Fellow with NPU, where he is currently an Associate Professor with the School of Marine Science and Technology. His research interests include sonar signal processing with distributed sensors and advanced sonar system designing.

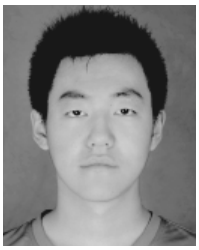

YAO ZHANG received the B.S. degree in underwater acoustic engineering from Northwestern Polytechnical University (NPU), Xi'an, China, in 2017, where he is currently pursuing the M.E. degree in underwater acoustic engineering with the School of Marine Science and Technology.

His research interests include forward scattering, and sonar signal processing and detection.

YIXIN YANG (M'03) received the B.S. degree in applied electronic engineering and the M.S. and Ph.D. degrees in underwater acoustic engineering from Northwestern Polytechnical University (NPU), Xi'an, China, in 1997, 1999, and 2002, respectively.

From 2002 to 2004, he was a Research Fellow with the School of Electrical and Electronic Engineering, Nanyang Technological University, Singapore. Since 2004, he has been with the School of Marine Science and Technology, NPU, where he became a Professor, in 2006. He is currently an Assistant President of NPU. His research interests include acoustic array signal processing, spectral estimation, and their applications.

Dr. Yang is a member of the Acoustical Society of America and the Chair of the Underwater Acoustics Committee of the Acoustical Society of China.